



## Device pattern impact on optical endpoint detection by interferometry for STI CMP

Sophia Bourzgui, Agnès Roussy, Jakey Blue, Gaëlle Georges, Emilie Faivre,  
Karen Labory

### ► To cite this version:

Sophia Bourzgui, Agnès Roussy, Jakey Blue, Gaëlle Georges, Emilie Faivre, et al.. Device pattern impact on optical endpoint detection by interferometry for STI CMP. International Conference on Planarization/CMP Technology, Oct 2017, Leuven, Belgium. hal-01622593

**HAL Id: hal-01622593**

**<https://hal.science/hal-01622593>**

Submitted on 31 Mar 2020

**HAL** is a multi-disciplinary open access archive for the deposit and dissemination of scientific research documents, whether they are published or not. The documents may come from teaching and research institutions in France or abroad, or from public or private research centers.

L'archive ouverte pluridisciplinaire **HAL**, est destinée au dépôt et à la diffusion de documents scientifiques de niveau recherche, publiés ou non, émanant des établissements d'enseignement et de recherche français ou étrangers, des laboratoires publics ou privés.

## Device pattern impact on optical endpoint detection by interferometry for STI CMP

S. Bourzgui <sup>1,2,3, a</sup>, A. Roussy <sup>1</sup>, J. Blue <sup>1</sup>, G. Georges <sup>2</sup>, E. Faivre <sup>3</sup>, K. Labory <sup>3</sup>, A. Allard <sup>3</sup>

<sup>1</sup>Mines Saint-Etienne and LIMOS, UMR CNRS 6158, CMP Georges Charpak, F-13541 Gardanne, France

<sup>2</sup>Aix Marseille Univ, CNRS, Centrale Marseille, Institut Fresnel, Marseille, France

<sup>3</sup>STMicroelectronics, Rousset, France

E-mail: [sophia.bourzgui@st.com](mailto:sophia.bourzgui@st.com)

*In this study, the focus is made on interferometry endpoint detection for Shallow Trench Isolation (STI) Chemical Mechanical Planarization (CMP) process done on the first platen of the tool for a three platen-polishing configuration. The interferometry principle is based on light interferences produced by thin transparent and semi-transparent layers. Thus the removed thickness can be correlated to the intensity measured over time. The optical signal received during the SiO<sub>2</sub> removal is affected by patterned wafers and pattern type. For STI stack, parameters like Gap Fill SiO<sub>2</sub> thickness, trench depth, pattern density and surface topology, could be involved in laser light diffraction and scattering. In some cases, these unwanted effects are stronger than the periodical signal of the removed SiO<sub>2</sub> layer thus, preventing from endpoint algorithm usage.*

*A correlation analysis has been performed based on experimental data between memory product layouts parameters and the response of raw signal detection. It confirms that the more sizable the Electrically Erasable Programmable Read-Only Memory (E<sup>2</sup>PROM) coverage is, the weaker and noisier the signal is. However, our experiment also shows that regardless of the SiO<sub>2</sub> thickness, a deeper trench will produce a more exploitable signal. In conclusion, perspectives for future experimentations are explored, in order to set up CMP optical endpoint detection by interferometry for a broader type of memory device patterns.*

**Keywords:** Planarization, Chemical-mechanical Polishing, optical endpoint, interferometry, STI CMP, device pattern.

### 1. Introduction

Many in-situ process control systems using different methods (optical, thermal, friction electrochemical, acoustic) have been developed to monitor platen-by-platen polishing time [1]. One of the most relevant process control widely used for CMP is optical endpoint detection, with a monochromatic laser [2] [3] or, a white-light source for advanced nodes [4]. Optical endpoint detection shows good results in compensating for wafer-to-wafer pre-CMP process thickness variations and reducing post-CMP process thickness variations compared to a process control based on polishing by a fixed time.

In this paper, the research is centered on the endpoint detection by interferometry for STI CMP process. In fact, the polishing time of almost all technologies in the production line of STMicroelectronics Rousset site is monitored by optical endpoint detection, except for a single category of products: 512kbits and more E<sup>2</sup>PROM memory chips. For those E<sup>2</sup>PROM memory

systems, the signal is noisier and the amplitude is weaker compared to standard logic products (Fig. 1). The objective is to understand better the signal shape in function of input and process parameters. In the first phase, for sake of completeness, the interferometry principle is explained. Additionally, a list of factors, that can impact the periodical signal of SiO<sub>2</sub> removal, is drawn up. Secondly, the focus is made on memory products, to better experimentally understand the signal response. A design of experiments of 25 runs combined three factors: E<sup>2</sup>PROM size, SiO<sub>2</sub> thickness, and depth trench. At last signal shapes correlations with the entry parameters will be analyzed. The conclusions to these experiments will give directions of future researches.

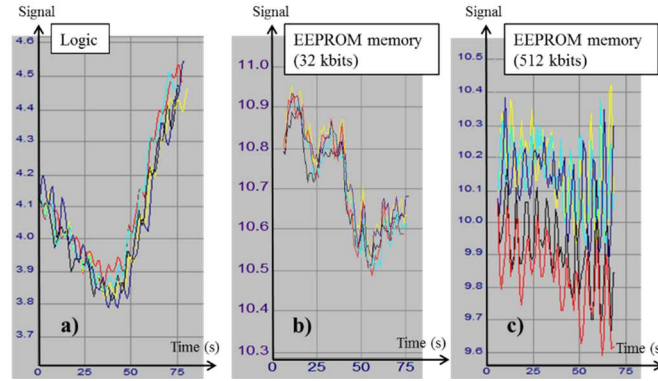


Fig. 1: The three graphs show 5 unfiltered signals of a) a logic product, b) 32kbits E<sup>2</sup>PROM product and c) 512kbits E<sup>2</sup>PROM memory product, each curve representing a wafer. The sinusoid corresponding to the SiO<sub>2</sub> layer removed over time is easily seen for a) and b). For the 512 kbits memory product, a noise with a period of about 5 seconds and high amplitude, prevents the detection of the SiO<sub>2</sub> thickness sinusoid.

## 2. Endpoint detection by interferometry

Endpoint detection by interferometry uses the properties of light interference caused by thin transparent and semi-transparent layers. Light interferences are obtained because SiO<sub>2</sub> layer thickness is about hundred nanometers scale, which is smaller than the laser beam diameter and reflected beams are superposed. For two reflected beams (Fig 2), the intensity detected is the addition of the intensity of the reflected beams by each layer (I<sub>1</sub> and I<sub>2</sub>) and an interference term function of I<sub>1</sub>, I<sub>2</sub> and of the phase difference  $\Delta\phi$  between the waves[5] written:

$$I = I_1 + I_2 + 2\sqrt{I_1 * I_2} * \cos \Delta\phi, \quad (1)$$

Additionally,  $\Delta\phi$  can be expressed as a function of the optical path difference  $\Delta p$  between the two waves, related to the material thickness  $d$  crossed by the incident light:

$$\Delta\phi = \frac{2*\pi}{\lambda} * \Delta p = \frac{2*\pi}{\lambda} * 2 * n * d * \cos \theta_1, \quad (2)$$

where  $\theta_1$  is the transmitted beam refraction angle. The refractive index  $n$  of removed material has to be known at the laser wavelength  $\lambda$ . Thanks to the equations (1) and (2), the SiO<sub>2</sub> thickness removal can be determined in function of the intensity detected over polishing time.

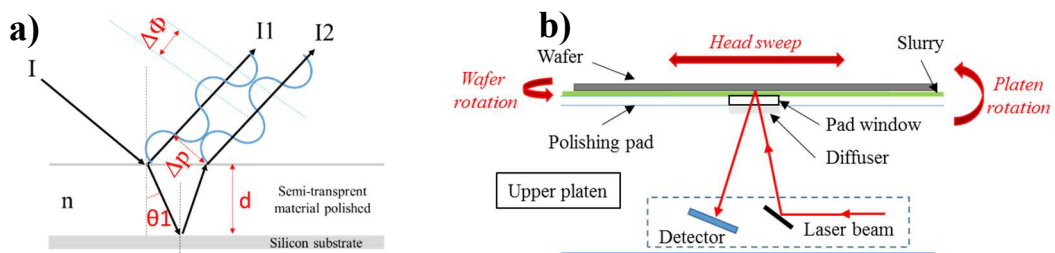


Fig. 2: a) depicts the interferometry principle for the simple case of two reflected beams on a SiO<sub>2</sub> layer above a silicon substrate. I is the incoming beam intensity from the laser source and it is both reflected on the semi-transparent material

surface and the bottom layer. As the two reflected beams come from the same source, they initially have the same phase at the origin, but a different phase after reflection, defined by the optical path difference  $\Delta p$ . b) represents a side view of the endpoint system located under the polishing platen.

For the CMP, many parameters disturb the sinusoidal signal corresponding to the  $\text{SiO}_2$  removed that can be split in two categories: CMP process factors and product design factors. CMP process factors include, movements of the rotating platen, the rotating head and the head sweep (Fig. 2b). Moreover, slurry particles can scatter the incident beam that reduce the detected intensity. However, these polishing recipe parameters do not change between technologies: slurry flow, head pressure, head and platen velocity are equal. Under these conditions, the significant difference of signal detection between logic and memory products (Fig. 1) can only be explained by entry process parameters and pattern device type.

### 3. Wafer pattern for memory products at active step

The signal is detected at the center of the wafer through a window of 45mm and an acquisition time of a few milliseconds. On the first platen, only the  $\text{SiO}_2$  removal is monitored and the objective is to leave about 100nm of  $\text{SiO}_2$  above the  $\text{Si}_3\text{N}_4$  layer, to obtain an optimal polishing process on platen 2. The signal detected is influenced by the following parameters:

- **The Gap Fill  $\text{SiO}_2$  surface topology:** it can cause the incident light to be reflected in random directions, thus rendering the outgoing signal weaker and noisier. This phenomenon can happen at the beginning of polishing until the process reaches the full  $\text{SiO}_2$  portion. The Gap Fill topology surface depends on trench depth and thickness.

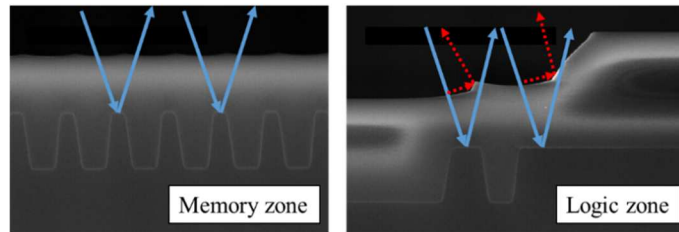


Fig. 3: The pictures represent cross sections of the Gap Fill deposition before STI CMP by Scanning Electron Microscopy (SEM) in two zones: memory and logic areas. The logic area has an uneven topology and varying trench widths, while the memory area is flat and trench width and spacing remain constant.

- **Gap Fill  $\text{SiO}_2$  thickness and the trench depth:** with a larger  $\text{SiO}_2$  thickness, the signal shifts to the right (Fig. 3a) and for a deeper trench, the signal amplitude decreases (Fig. 3b).

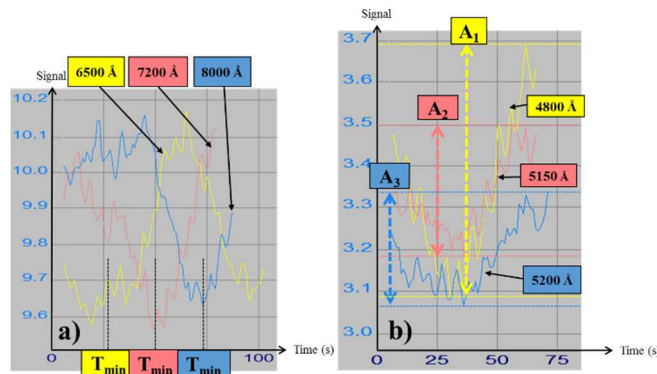


Fig. 4: On both graphs, each curve represents a wafer of the same product. a) depicts that with identical removal rates, pre-CMP process thickness variations cause the signal to shift over time. We can see that  $T_{\min}$ , the time at which the signal intensity is the lowest, shifts to the right with thickness increases. In b) each wafer has a different trench depth: with the same removal rate, pre CMP process trench depth variation impact the signal amplitude  $A_n$ . In this case,  $A_1 > A_2 > A_3$ , which means that the lower the trench, the higher the amplitude.

- **The pattern type and the density:** For some memory products, the use of an endpoint algorithm is already implemented in production. For these products (cf. Table 1) is that the E<sup>2</sup>PROM's size is no larger than 256 Kbits and no larger than 9% of the chip's surface. By comparing logic and memory products on Table 1, Gap Fill and trench depth do not highlight any relevant difference to explain the signal endpoint degradation issue. Likewise, the size of the Active Open Area for all products is within the specifications. The underlying factors causing a significant difference between products are the E<sup>2</sup>PROM size, the coverage of the E<sup>2</sup>PROM on the die, the number of dies per wafer: chip number decreases as the E<sup>2</sup>PROM size rises. The specificity of the E<sup>2</sup>PROM design is that the memory matrix is like a grid of SiO<sub>2</sub> trenches that has a higher density compared with logic zones.

Technology	Memory products					Logic products	
Products	A	B	C	D	E	F	G
Method used on platen 1	By endpoint	By endpoint	Constant time	Constant time	Constant time	By endpoint	By endpoint
Coverage E <sup>2</sup> PROM (%)	2.4	8.8	12.0	13.4	19.3	1.3	1.4
E <sup>2</sup> PROM size (kbits)	32	256	512	1024	2048	8	8
Dies number/wafer	30886	16248	11477	6573	4023	10026	56239
Coverage product (%)	46.6	37.9	34.8	31.5	32.1	40.1	36.6
Active Open Area	58.5	59.1	59.3	61.1	62.0	61.0	65.0
Coverage dummies (%)	0.4	1.2	0.9	1.6	0.2	1.1	9.4
Gap Fill thickness (Å)	6500	6500	6500	6500	6500	6130	6500
Trench depth (Å)	5750	5750	5750	5750	5750	5000	5750
Ratio Thickness/Trench	1.13	1.13	1.13	1.13	1.13	1.23	1.13

Table 1 lists the key of certain memory and logic products. In the memory products section, we notice that the Gap Fill thickness and the trench depth are equal for all products.

In order to highlight the three points of this section, a Design Of Experiment (DOE) is set up with the following factors: Gap Fill SiO<sub>2</sub> thickness, trench depth, and E<sup>2</sup>PROM size.

#### 4. Experiments

The objective of this study is to analyze how the signal is impacted by the variation of incoming parameters for E<sup>2</sup>PROM products. Repeatability and reproducibility have not been tested in this experiment but will be assessed in at a later date time on exploitable signals. Considering a maximum of 25 wafers available, those parameters have been tested on three levels as follow:

E <sup>2</sup> PROM size (kbits)	32	512	2064
Gap Fill thickness (Å)	6500	7200	8000
Trench depth (Å)	5350	5750	6150

Table 2: Input factors of the experiments to analyze their influence on the interferometric signal shape on platen 1

To study the E<sup>2</sup>PROM size influence, three memory products have been selected including one with a functional algorithm. The STI CMP process needs to respect a certain ratio between the trench depth and the SiO<sub>2</sub> thickness, large enough to enable a good planarization and to avoid a dishing effect in the non-dense zone of SiO<sub>2</sub> [6]. This has driven the choice of the different selected thicknesses for the experiment. Moreover, the trench's depth factor studies the impact on amplitude variation, seen in Fig. 4b. Finally, the influence of surface topology has been tested, by combining different trench depths and SiO<sub>2</sub> thicknesses.

In order to trace a signal long enough to configure an algorithm, wafers were polished with a fixed duration that including over-polishing. Furthermore, the data collection was made with no filters to be sure that the signal treatment is done properly on raw data. The goal is to have the same response during the algorithm development and real polishing conditions. To assess the Removal Rate (RR) of the tool, post measurement via off-line metrology ellipsometry tool

was made on a single wafer per E<sup>2</sup>PROM size, after polishing, in order to calculate the polishing time needed for platen 1.

## 5. Results

In our case of a limited number of 25 wafers, a D-Optimal experimental design has been selected. Considering the SiO<sub>2</sub> thickness and trench depth factors, the values used to study the influence are the theoretical values. In fact, only a part of the wafers was measured in line for a concern of costs and availability of metrology tools. The interferometric signal response characteristic are defined as follow (Fig. 5): signal peak-to-peak amplitude,  $T_{\min}$ : the time at which the signal intensity is the lowest and  $T_{\max}$ : the time at which the signal intensity is the highest, periodical noise amplitude and signal level intensity. For a better precision of the responses concerning the signal characterization, specific filters were used for each response category.

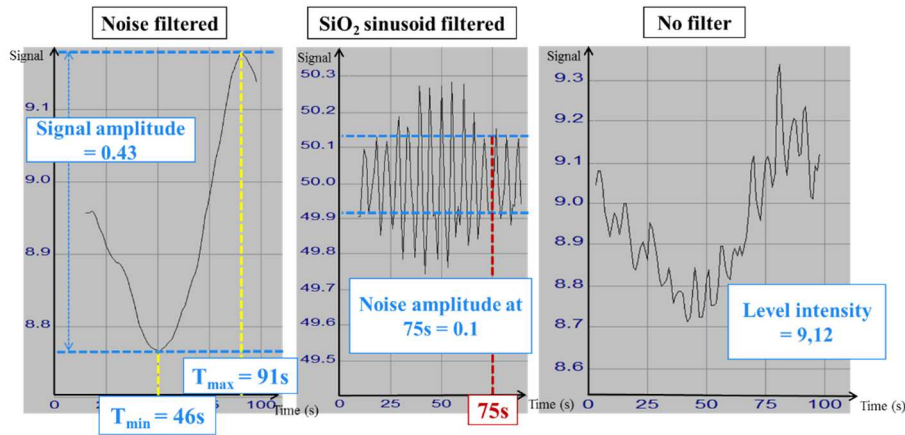


Fig 5: Responses associated with the D-Optimal plan.  $T_{\min}$ ,  $T_{\max}$  and the signal amplitude are determined from the SiO<sub>2</sub> removal curve with noise filtering. On the contrary, the noise amplitude is given by filtering the SiO<sub>2</sub> removal curve. Finally, the intensity level is determined without any filter

The signal level intensity results, deduced by the value given by the software used for algorithm development, implied that the smaller the E<sup>2</sup>PROM size is, the higher the intensity. The signal peak-to-peak amplitude is characterized by filtering the periodical noise. The model shows that the trench depth and the SiO<sub>2</sub> thickness have an impact on this parameter (Fig. 6). The signal amplitude decreases for a trench depth value around 5750Å and increases at the edge of the domain for a 5350Å and 6150Å trench depth. The noise amplitude is defined by filtering each signal with a period to enhance filter of 5 seconds, corresponding to the average period of periodical noise for all curves. The filter erases the SiO<sub>2</sub> layer sinusoid and only the noise is visible. As expected, this parameter is influenced by E<sup>2</sup>PROM size, increasing with the biggest ones, but it is also influenced by the trench depth, the noise amplitude is the highest for the smaller one. Finally, the signal positioning over time is represented by  $T_{\min}$  and  $T_{\max}$ . On one hand, the  $R^2$  of  $T_{\min}$  response is weak (Table 3), which probably means that this parameter was not correctly measured. On the other hand, the  $T_{\max}$  responses has a very good  $R^2$  and  $R^2_{\text{adjusted}}$  associated with a simple linear model which confirms that the SiO<sub>2</sub> thickness is the most influential factor on the positioning of the signal minimum and maximum amplitude.



Responses	R <sup>2</sup>	R <sup>2</sup> <sub>adjusted</sub>	Influent factors	Model
Level intensity	0.97	0.96	E <sup>2</sup> PROM / trench depth	Quadratic
Signal amplitude	0.896	0.86	Trench depth / SiO <sub>2</sub> thickness	Quadratic
Noise amplitude	0.82	0.78	E <sup>2</sup> PROM / trench depth	Quadratic
T <sub>min</sub>	0.78	0.70	Trench depth / SiO <sub>2</sub> thickness	Square root
T <sub>max</sub>	0.97	0.965	E <sup>2</sup> PROM / trench depth / SiO <sub>2</sub> thickness	Linear

Table 3: Summary table of the experimental plan analysis. The models are calculated using the variance analysis method (ANOVA) taking into account the p-value terms less than 5%. The lower R<sup>2</sup> of the signal amplitude and T<sub>min</sub> responses can be induced by the fact that five results are missing, because on certain curves the minimum amplitude is not distinguishable

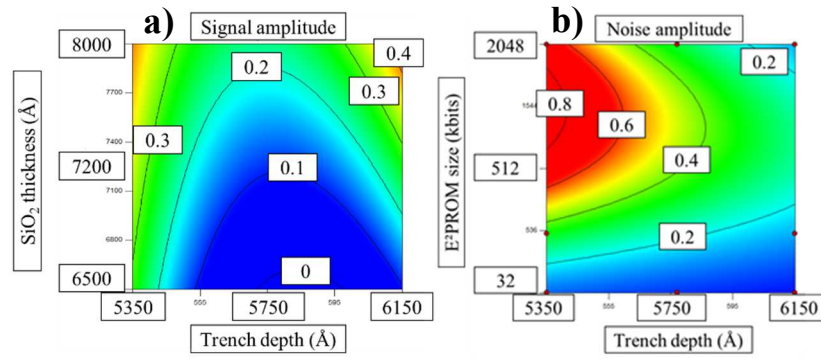


Fig. 6: The response surfaces of a) the signal amplitude and b) the noise amplitude versus their influent factors. To determine the optima in terms of the value of SiO<sub>2</sub> thickness and trench depth for the large E<sup>2</sup>PROMs, it is expected that the amplitude should be as large as possible and the Noise amplitude to be as low as possible.

## 6. Conclusions and perspectives

In summary, how the memory product parameters affected the signal is studied in this paper. Our next step will be to classify the level of parameters and to define with which configuration the raw signal is exploitable for proper filtering. For example, and contrary to the experimental domain of depth trench seen in Fig. 4, these experiments show that for a deeper trench, the signal-to-noise ratio is improved and the signal shape is close to what it is expected: a clear distinction of the SiO<sub>2</sub> sinusoid. Moreover, combined to the bigger Gap Fill, the sinusoid shape presents a complete half period, compared with the other Gap Fill that could help set an endpoint window easily. In addition, with these two parameters, the thickness-trench ratio is respected. The second step will be, with available raw signals, to find a robust algorithm with efficient filters to support an endpoint. The essential element of an endpoint algorithm is that its repeatability and reproducibility are verified. Thus, algorithms have to be tested on more wafers to validate the endpoint detection robustness. In parallel, in order to make a deeper analysis on the optical phenomenon produced by the different positions of pattern wafers, a comparative study of the laser light behavior through different E<sup>2</sup>PROM size with different laser wavelengths will be set up. A better understanding of the observed signal noise origin for the biggest E<sup>2</sup>PROM sizes is expected.

## 7. References

- [1] Hetherington, Dale L., and David J. Stein. *In-line monitoring of chemical-mechanical polishing processes*. Microelectronic Manufacturing'99. International Society for Optics and Photonics, 1999.
- [2] Fang, S. J., et al. *Control of dielectric chemical mechanical polishing (CMP) using an interferometry based endpoint sensor*. Interconnect Technology Conference, 1998. Proceedings of the IEEE 1998 International. IEEE, 1998.
- [3] Chan, David A., et al. *Process control and monitoring with laser interferometry based endpoint detection in chemical mechanical planarization*. Advanced Semiconductor Manufacturing Conference and Workshop, 1998. 1998 IEEE/SEMI. IEEE, 1998.
- [4] Perrot, C., et al. *STI CMP stop in Silicon Nitride controlled by FullVision TM endpoint*. Planarization/CMP Technology (ICPT 2012), International Conference on. VDE, 2012.
- [5] Hariharan, Parameswaran. *Basics of interferometry*. Academic Press, 2010.
- [6] Li, Yuzhuo, ed. *Microelectronic applications of chemical mechanical planarization*. John Wiley & Sons, 2007.